A Macrokinetic Approach to Crystallization Applied to a New Thermoplastic Polyimide (New TPI) as a Model Polymer

LUIGI TORRE,[1] ALFONSO MAFFEZZOLI,[2,*] and JOSÉ M. KENNY[3]

[1]Department of Materials and Production Engineering, University of Naples "Federico II," P. Tecchio, 80125, Naples, [2]Department of Materials Science, University of Lecce, Via per Arnesano, 73100, Lecce, and [3]Institute for Chemical Technologies, University of Perugia, Loc. Pentima Bassa, 21-05100 Terni, Italy

SYNOPSIS

The application of a new macrokinetic approach to polymer crystallization is applied in this work to a new thermoplastic polyimide (New TPI) recently developed as a matrix of advanced polymer matrix composites. The slow crystallization kinetics presented by New TPI in the entire range between the glass-transition temperature and the melting point makes TPI an excellent model polymer for testing crystallization models. In the approach presented here the variation of the induction time with the temperature is included in the Nakamura model for nonisothermal crystallization, and a simplified expression of the kinetic constant as a function of the temperature is adopted. The proposed model is verified through a comparison with a complete set of experimental data, ranging from the melting point to the glass-transition temperature of the polymer, obtained in isothermal and nonisothermal conditions. Moreover phase transformation diagrams (TTT and CCT plots) are presented, providing a fundamental tool for understanding the crystallization behavior of semicrystalline matrices and to determine the more appropriate processing conditions. © 1995 John Wiley & Sons, Inc.

INTRODUCTION

The analysis of the development of crystallinity during the processing of semicrystalline polymeric materials requires the application of a macrokinetic approach to describe the dependence of the degree of crystallization on time and temperature. Although the kinetics of polymer crystallization has been studied for a long time from the microscopic and macroscopic points of view,[1,2] many theoretical and experimental questions remain to be solved as a consequence of the complexity of the nucleation and growth phenomena of macromolecular crystals. In particular, the melting history of a polymer can modify the crystallization kinetics acting on the nucleation process or altering the polymer structure due to branching, partial crosslinking, degradation phenomena, or destruction of self-nucleation sites.[3,4] In the case of advanced composite materials the effect of the fibers on the matrix crystallization phenomena must be considered. Fibers may act on crystallization as nucleating agents, modifying the crystal growth, and reducing the maximum degree of crystallinity as a consequence of the steric hindrance offered to crystal growth.[5,6]

From the experimental point of view, as a consequence of the restrictions of the most common available techniques (X-ray, calorimetry, and dilatometry), the crystallization kinetics of most of the semicrystalline polymers can be normally analyzed only in a narrow temperature interval and under low cooling rates. This effect has been extensively reported for typical matrices for high performance semicrystalline matrices such as (PPS) polyphenylene sulfide and polyetherether ketone (PEEK).[7-12] However, among the most recently developed thermoplastic polymers, a new thermoplastic polyimide, called New TPI, is characterized by a crystallization

* To whom correspondence should be addressed.

Journal of Applied Polymer Science, Vol. 56, 985-993 (1995)
 CCC 0021-8995/95/080985-09

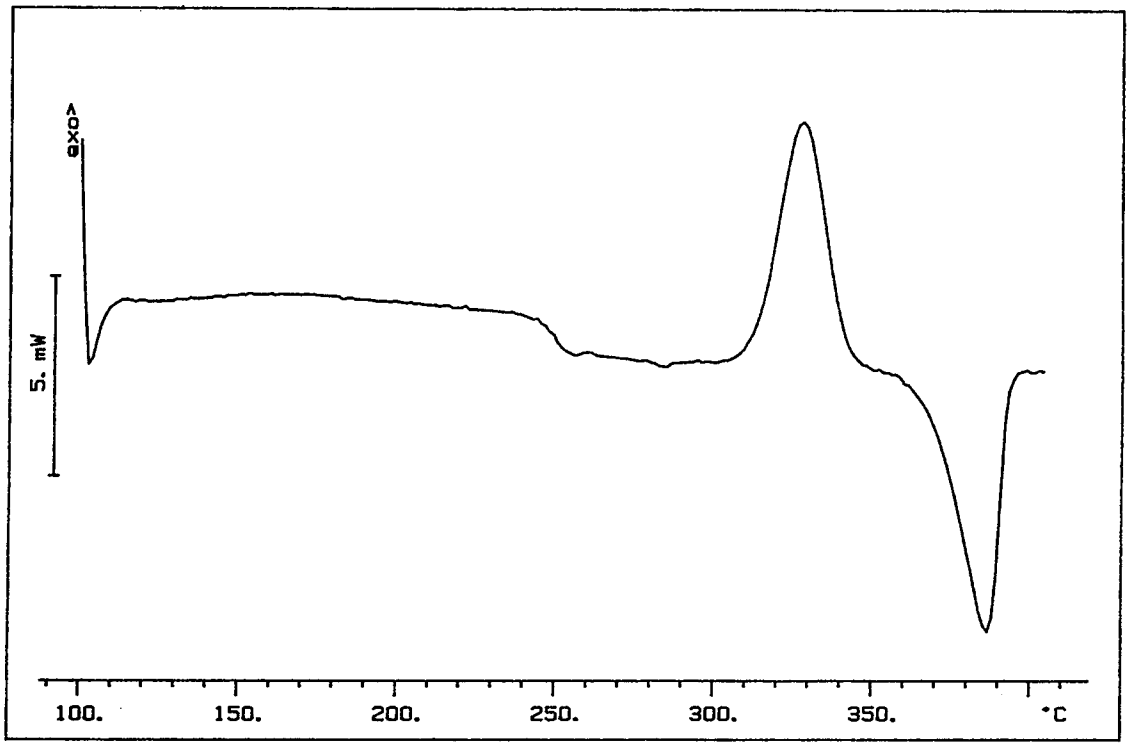

Figure 1 Dynamic scan obtained on the material as received.

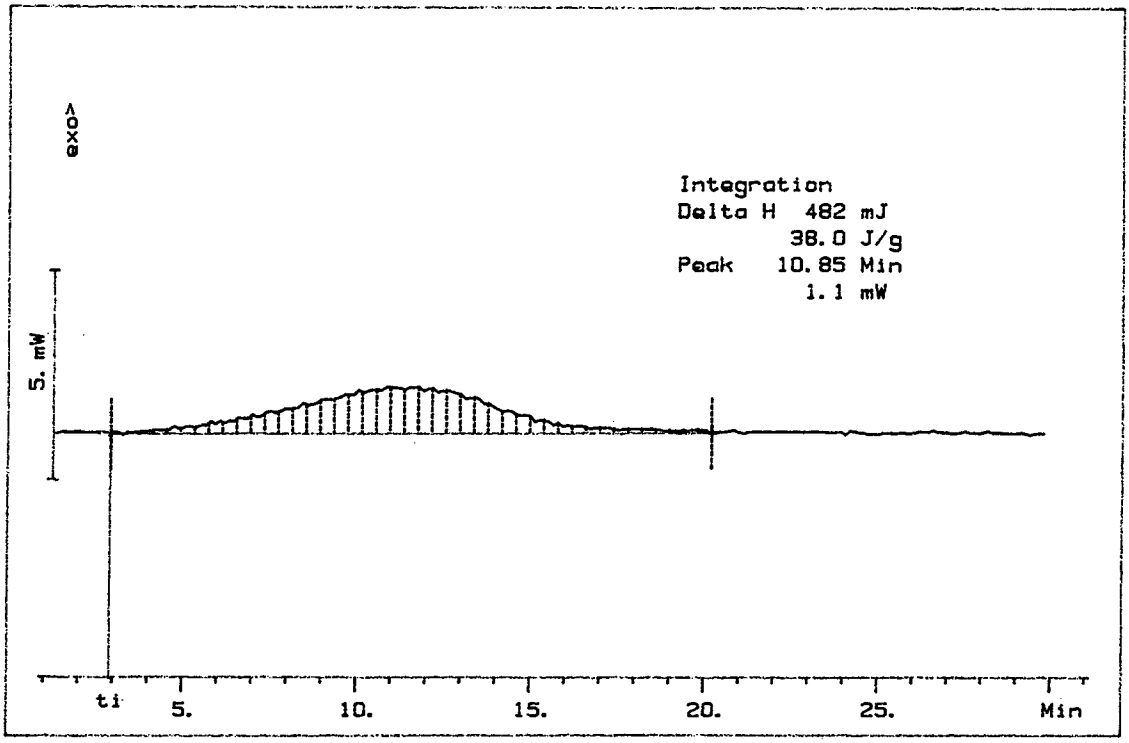

Figure 2 Isothermal DSC thermogram obtained during melt crystallization at 360°C. t_i represents the induction time.

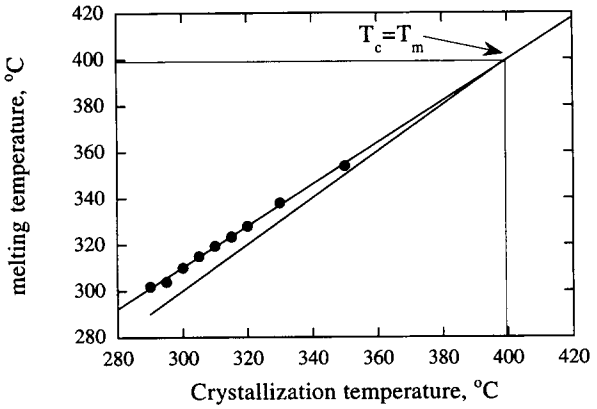

Figure 3 Experimental determination of T_m^0.

process that is relatively slow compared with that of most common thermoplastic matrices. It can be used as a model system for testing crystallization models in isothermal and nonisothermal conditions across the overall crystallization range including quenching effects.

The first thermoplastic polyimide was developed by NASA and patented under the name of LARC TPI[13]; this resin presented thermoplastic behavior and a lower processing temperature with respect to conventional polyimides.[13,14] Later Mitsui Toatsu Inc. modified LARC TPI and patented the New TPI.[15] A grade of this resin was used in this work. The crystallization behavior of New TPI was studied by Hou and Reddy,[16] Hou et al.,[17] and Friler and Cebe,[18] using differential scanning calorimetry (DSC), X-ray scattering, and dynamic mechanical tests. The kinetic studies performed by those authors showed a finite crystallization rate in the whole interval between the glass-transition temperature (T_g) and the melting point (T_m) that followed an Avrami

Table I Parameters Obtained from Avarmi Analysis

Temp. (°C)	n	$\ln(k)$ (s^{-n})
290	2.07	−14.45
295	2.09	−13.77
300	2.15	−13.20
305	2.01	−11.70
310 (cold cryst.)	2.07	−11.60
310 (melt cryst.)	2.05	−11.30
315	1.96	−10.77
320	2.03	−10.52
330	1.99	−10.30
340	2.10	−10.72
350	2.10	−11.70
360	2.13	−13.32

kinetic model. Although some modeling approach was applied in those studies, no quantitative comparison of experimental and modeling results was presented.

The study of the crystallization kinetics of polymers under different thermal conditions is very important for the analysis and design of processing operations. In fact, during fabrication the polymeric material suffers one or more cycles of heating, melting, cooling, and crystallization that determine the development of the polymer structure and the physical properties of the final product. Usual processing conditions may involve cooling rates capable of partially quenching the polymer, introducing dishomogeneity in the formed parts, and significantly affecting the mechanical properties and the thermal and environmental resistance.[5,19,20] This problem has been previously addressed[7,8] through the application of a new kinetic model, based on a modified Kamal

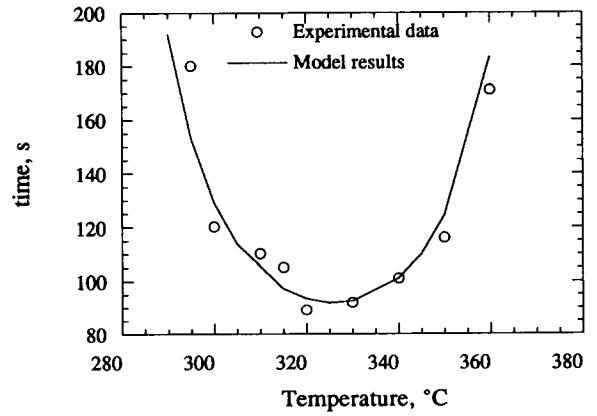

Figure 4 Temperature dependence of induction times obtained during isothermal crystallization.

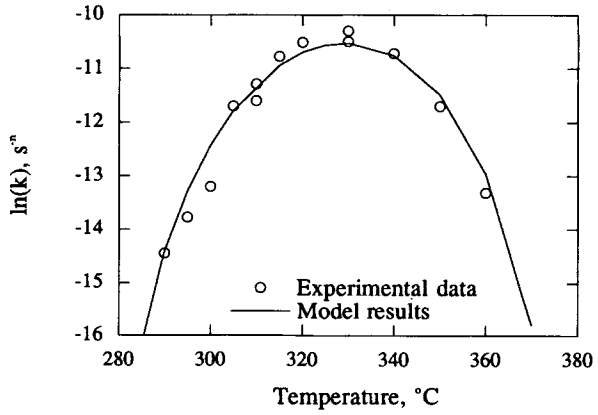

Figure 5 Temperature dependence of kinetic constants calculated during isothermal cold and melt crystallization.

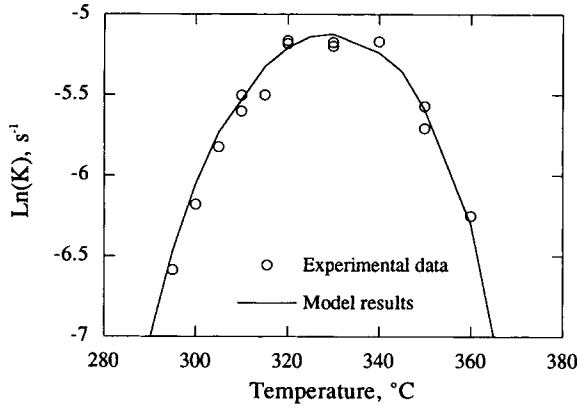

Figure 6 Kinetic constants normalized by the Avrami index obtained during each isothermal crystallization.

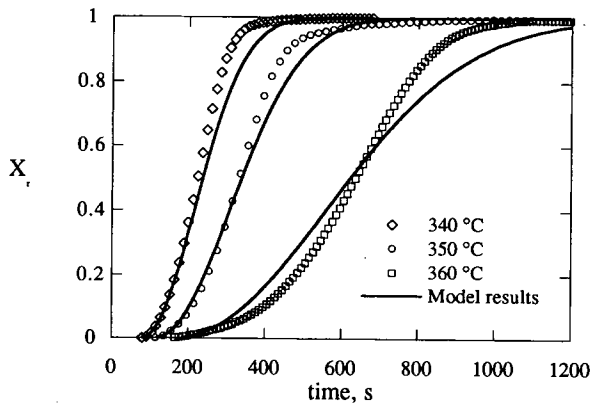

Figure 7 Comparison between experimental data (points) and model predictions (lines) during isothermal crystallization.

equation,[21] to the crystallization of PPS and PPS matrix/carbon fiber composite. The model included the effects of nucleation and a simplified expression for the kinetic constant was proposed. Moreover, the overall crystallization behavior was summarized in time temperature transformation (TTT) plots and continuous cooling transformation (CCT) plots for processes conducted in isothermal and continuous heating conditions, respectively. Although the results obtained with PPS were encouraging, only experimental data obtained in a narrow range around T_g and T_m were obtained as a consequence of the very fast crystallization rates in the rest of the interval. Thus the new proposed approach still needs a full validation on experimental data covering the overall temperature range. In this work a theoretical and experimental study of the crystallization kinetics of the New TPI is presented. The crystallization process is analyzed by calorimetry in isothermal conditions by cooling from the melt and by annealing the originally amorphous polymer at temperatures above T_g. Different crystallization models are then compared and TTT and CCT plots are presented, providing a fundamental tool to describe the crystallization behavior of semicrystalline matrices, and to determine the more appropriate processing conditions.

Table II Parameters of Kinetic Model

$\ln(k_{0n}) = 0.33\ s^{-1}$	$E_{1n}/R = 176$ K	$E_{2n}/R = 235$ K
$T_g = 249$°C	$T_m^0 = 399$°C	$n = 2.06$
$\ln(k_{t0}) = 1.955$ s	$E_{t1}/R = 91.5$ K	$E_{t2}/R = 101$ K
$X_{rmax} = 0.27$		

EXPERIMENTAL

Calorimetric tests were performed on samples of New TPI #450 quenched film using a differential scanning calorimeter Mettler DSC 30. The film was dried for 24 h at 100°C before each test. The thermal behavior of the material as received is shown in the DSC thermogram reported in Figure 1. The glass transition, the cold crystallization, and the melting processes are evident and their temperature intervals correspond to those reported previously.[17]

The same material was analyzed in isothermal melt and cold crystallization tests. The samples for the melt crystallization were kept at 400°C for 5 min and then quenched at 100°C/min to the temperature of the isothermal crystallization. These experiments were performed in a range of temperatures between 290 and 360°C. A typical isothermal test is reported in Figure 2 where it is possible to observe

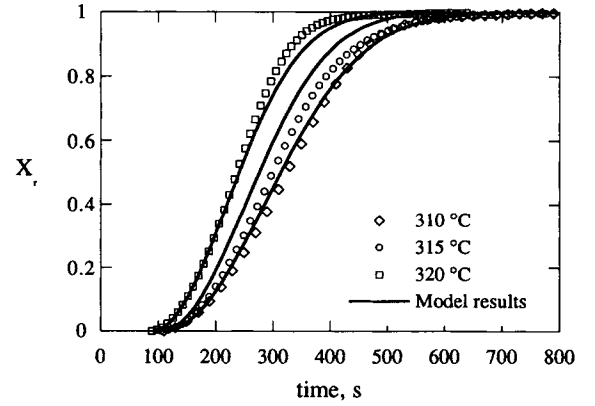

Figure 8 Comparison between experimental data (points) and model predictions (lines) during isothermal crystallization.

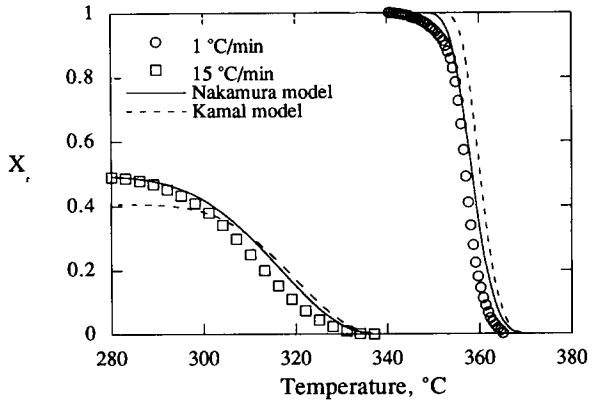

Figure 9 Comparison between the Nakamura and Kamal model predictions at different cooling rates.

smooth crystallization kinetics with a clearly detected induction time before crystallization starts. Moreover, experiments for partial quenching were performed in the DSC keeping the sample at 400°C for 5 min and then cooling at a temperature below T_g using several different cooling rates in order to produce samples with different crystallinity fractions.

Dynamic tests after each isothermal crystallization were performed at 10°C/min and a double melting peak was always detected with the smaller peak occurring in the temperature interval close to the temperature of the previous isothermal process. This fact, already reported for different semicrystalline thermoplastic polymers can be applied to the extrapolation of the theoretical melting temperature (T_m^0), as shown in Figure 3, accordingly with the procedure described by Hoffman et al.[2] A value of T_m^0 = 399°C, close to that reported by Huo et al.,[17]

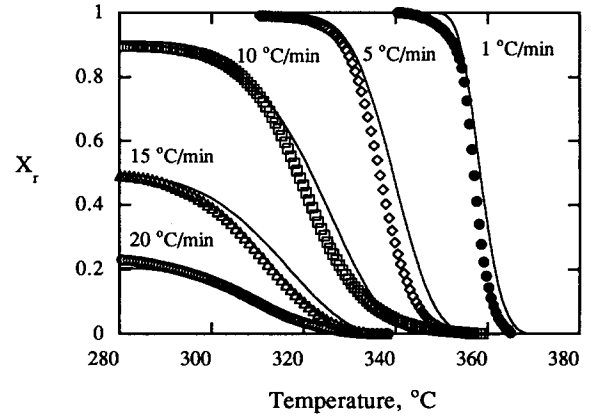

Figure 10 Comparison between experimental data (points) and Nakamura model predictions (lines) during crystallization at constant cooling rate.

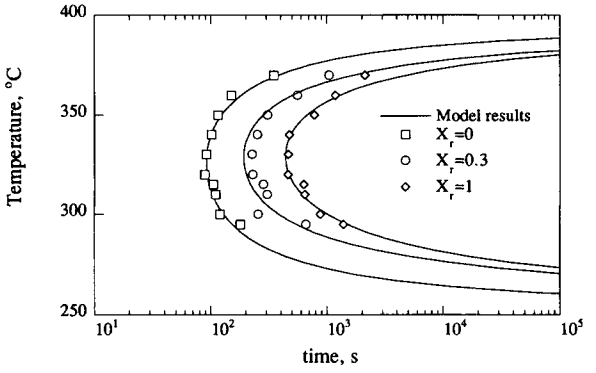

Figure 11 Experimental data and model predictions on a time–temperature-transformation diagram.

was calculated. A T_g = 249°C was measured (Fig. 1); the heat of fusion of a perfect crystal, H_f = 139.4 J/g, and the densities of the amorphous phase, r_a = 1.333 g/cm^3, and of the crystalline phase, r_c = 1.455 g/cm^3, were taken from the literature.[18] The values of H_f, r_a, and r_c were used to obtain the values of volume fraction crystallinity from the DSC data as described in a previous article.[5]

RESULTS AND DISCUSSION

Isothermal crystallization

The macrokinetics of the isothermal crystallization of semicrystalline polymers, extensively reported in the scientific literature,[1] can be typically represented by the Avrami equation:

$$X_r(t) = 1 - \exp(-kt^n) \quad (1)$$

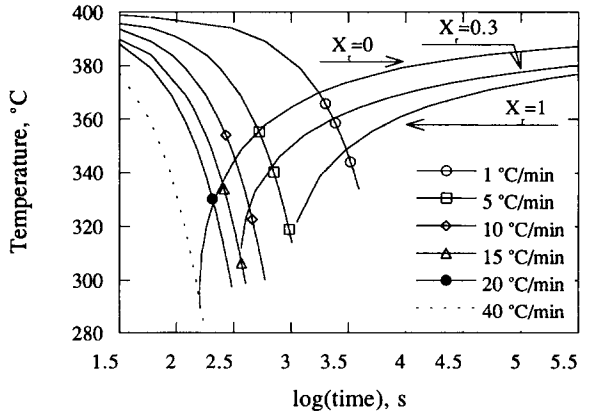

Figure 12 Experimental data and Nakamura model predictions on a constant-cooling-transformation diagram.

where X_r is the relative volume fraction of crystallinity referred to as the maximum amount of developed crystallinity, n is the Avrami exponent, and k is the kinetic constant. However, the model reported above can be applied only to crystal growth after nucleation. In fact, heterogeneous and homogeneous nucleation are thermally activated phenomena and their effects can be macroscopically detected by isothermal DSC experiments (Fig. 2) where the exothermal heat signal during the crystallization can be observed only after a delay (induction time), attributed to the formation of nuclei of critical size.[5,7,8] The induction time cannot be directly detected in nonisothermal crystallization experiments but it plays a fundamental role determining the onset time for the crystal growth. Therefore a prediction of a full quenching of the polymer during fast cooling is not possible without considering the induction time. Further, the induction time may be considered as the most suitable macroscopic parameter representative of the nucleation process in calorimetric experiments. The temperature dependence of the induction time (t_i) previously proposed[7,8] is adopted in this study:

$$t_i = 1\Big/\left[K_{t0}\exp\left[\frac{-E_{t2}}{R(T-T_g)}\right]\exp\left[\frac{-E_{t1}}{R(T_m^0-T)}\right]\right]. \quad (2)$$

Induction times obtained in isothermal DSC experiments performed at different temperatures were used to compute the parameters of eq. (2) by nonlinear regression. Although the fast crystallization process of PPS previously studied[7,8] strongly limits the temperature range in which t_i can be measured, for TPI the induction times can be properly measured across the overall crystallization range (Fig. 4) and a good agreement between experimental data and eq. (2) predictions is observed.

Once the crystallization time is scaled by the induction time, the parameters of the Avrami model can be calculated using the classical double logarithm method on both sides of eq. (1).[1] The values of n and k are also reported in Table I for the cold and melt crystallization experiments. Moreover, Figure 5 shows the characteristic bell-shaped curve representing the complex behavior of the kinetic constant in the interval between T_g and T_m^0. Because the rate of crystallization is zero at the glass-transition temperature and at the melting point, $1/(T_m^0 - T)$ may be assumed as a thermodynamic driving force for crystallization and $1/(T - T_g)$ as a diffusion controlled driving force accounting for the increase of viscosity when the temperature approaches T_g. Then, the simplification of the classical temperature dependence of k, previously proposed,[7,8] can be adopted:

$$k = k_0\exp\left(-\frac{E_2}{R(T-T_g)}\right)\exp\left(-\frac{E_1}{R(T_m^0-T)}\right). \quad (3)$$

The physical dimensions of k, $[s^{-n}]$, are dependent on the value of the Avrami exponent. Although some differences among the exponents calculated at different isothermal temperatures can be observed (see Table I), k is generally plotted as a function of the temperature (Fig. 5). However, following a more rigorous approach the kinetic constants should be corrected at each temperature by the corresponding values of n and thus reported to $[s^{-1}]$ in the following form:

$$K = k^{1/n} = \left[k_0\exp\left(-\frac{E_2}{R(T-T_g)}\right) \times \exp\left(-\frac{E_1}{R(T_m^0-T)}\right)\right]^{1/n}. \quad (4)$$

Now, the behavior of K as a function of the temperature, reported in Figure 6, displays a lower scattering compared with the values of k shown in Figure 5. Because n can be considered as independent of temperature, taking $K_{0n} = k_0^{1/n}$, $E_{1n} = E_1/n$ and $E_{2n} = E_2/n$, K can be expressed as:

$$K = K_{0n}\exp\left(-\frac{E_{2n}}{R(T-T_g)}\right) \times \exp\left(-\frac{E_{1n}}{R(T_m^0-T)}\right). \quad (5)$$

The values of K, obtained from isothermal DSC experiments performed at different temperatures, were used to compute the parameters of eq. (5) by nonlinear regression. A good agreement between model predictions and experimental values is observed in Figure 5. Moreover an average value of $\bar{n} = 2.05$ was calculated, by nonlinear regression analysis, from eq. (4). With this value it was possible to compute E_1, E_2, and k_0 and to compare the predictions of eq. (3) represented in Figure 5 as a solid line. The complete set of parameters of the kinetic model is reported in Table II. As in the case of the induction times, the kinetic constant can be measured for the New TPI along the overall crystallization range (Figs. 5, 6).

The predictions of eqs. (1), (2), and (3) are com-

pared with isothermal melt and cold crystallization experimental results in Figures 7 and 8 using the parameters of Table II, including the Avrami exponent. The onset of crystallization is well predicted by the induction time model in these experiments indicating that the nucleation process is correctly represented by the proposed macrokinetic approach. The moderate mismatch between the model and the experimental data can be explained in terms of the typical intrinsic scattering of DSC results and of the variability of the values of n.

Nonisothermal Crystallization

The nonisothermal crystallization has been traditionally approached starting from the classical Avrami model [eq. (1)] and obtaining integral or differential models with a temperature dependent kinetic constant.[21-24] Among the empirical expressions, the model of Kamal and Chu[21] is expressed in its differential form by Lin[22] as:

$$\frac{dX_r}{dt} = nk(T)(1 - X_r)t^{n-1}. \tag{6}$$

This model can be reduced to the classical Avrami equation [eq. (1)] in isothermal conditions. On the other hand Nakamura et al.[23] proposed the following integral expression extending the general Avrami theory to nonisothermal conditions:

$$X_r(t) = 1 - \exp\left[-\left(\int_0^t K(T)\,dt\right)^n\right]. \tag{7}$$

$K(T)$ is given by eq. (5). Evidently also eq. (7) reduces to the Avrami equation under isothermal conditions.

In order to integrate these expressions, an initial condition, giving the temperature T_i at which $t = 0$, must be provided. The initial condition in a nonisothermal simulation is given by the induction time calculated as the sum of the contributions of isothermal temperature steps. Then the nonisothermal induction time, t_{ni}, may be computed in terms of a dimensionless parameter Q, ranging from 0 to 1, defined as:

$$Q = \int_0^{t_{ni}} \frac{dt^*}{t_i} \tag{8}$$

where t_i is the isothermal induction time given by eq. (2). Numerical integration of eq. (8) is performed taking $t^* = 0$ at the melting temperature (T_m^0). The value $t^* = t_{ni}$ at which Q reaches the unity represents the nonisothermal induction time.

At this point, the initial condition for the integration of eqs. (6) and (7) at constant cooling rate (V) is given by:

$$Q = 1 \quad t = 0 \quad T_i = T_m^0 - Vt_{ni}. \tag{9}$$

The nonisothermal crystallization models, given by eqs. (6) and (7), were tested in constant cooling rate experiments using the parameters obtained from the analysis of the isothermal data reported in Table II. The induction time and the kinetic constants were calculated by eqs. (2)–(5), (8), and (9). The comparison between the Nakamura and the Kamal model presented in Figure 9, gives interesting indications about the validity of the model. Even though both models work well at low cooling rates, it can be noted that the Nakamura model does a better job of representing the experimental data at cooling rates approaching the partial quenching of the polymer. In previous articles[7,8] the Kamal model gave good performances because it was tested at low cooling rates compared with the very high cooling rates needed to quench PPS.

Finally, the ability of the Nakamura model [eq. (7)], coupled with the proposed expressions for t_i and K [eqs. (2)–(5)], to represent the experimental data in nonisothermal conditions is shown in Figure 10 over a broad range of cooling rates. It must be noted that, due to the slow crystallization process of New TPI, it was possible to successfully test the validity of the model also at cooling rates close to the quenching condition.

Phase Transformation Diagrams

The crystallization kinetic model presented previously, can be exploited for the development of phase transformation diagrams like TTT plots for isothermal processes and CCT plots obtained at constant cooling rates. These plots are widely used for the study of solid-state phase transformations governed by slow kinetic processes.[25] The same kind of approach has been used by Enns and Gillham[26] for the chemorheology of thermosetting matrices, in order to predict gelation and vitrification phenomena during cure of composite matrices. In previous works[7,8] these plots, presented for the crystallization kinetics of polymers, were essentially developed based on the results of a kinetic model.

The crystallization behavior of the polymer used in this research and the kinetic model proposed in this article can now provide experimental and theo-

retical evidences to build quantitative TTT and CCT plots. The crystallinity content as a function of the cooling rate can be reported as a fundamental tool for process design and optimization. In Figures 11 and 12 experimental data and theoretical results are combined in order to construct a TTT and a CCT diagram, respectively. The points reported in these figures at $X_r = 0$ corresponds to the nonisothermal induction time; at $X_r = 0.3$ and $X_r = 1$ the points are representative of the DSC experimental results. The development of crystallinity as a function of time on a TTT plot can be determined as the intersection of the isothermal horizontal line with the curve representing the locus of the points of the constant degree of crystallinity. On the other hand, on a CCT plot the development of crystallinity as a function of time and temperature is obtained by following a constant cooling rate curve. The time required for $X_r = 1$ is infinite, then the curve corresponding to full crystallization has been calculated for $X_r = 0.99$. It must be pointed out that these plots can be rigorously used only for isothermal (TTT) and constant-cooling rate (CCT) processes. For more complex thermal conditions, the model must be integrated in order to obtain a time–temperature plot.

Moreover, the CCT plot, including the nucleation behavior, can be used to predict the full quenching of the New TPI composite matrix when the continuous cooling curve does not intersect the curve representative of the onset of crystallization ($X_r = 0$). In particular, Figure 12 indicates that the limiting quenching rate is 40°C/min. An experimental verification of this result is provided by the DSC experiment at 30°C/min characterized by a very small and broad exothermic peak, indicating that a very limited crystal growth has occurred. Further, the CCT plot indicates that the limiting cooling rate for full crystallization is about 5°C/min.

CONCLUSIONS

The slow crystallization process of new TPI has been exploited in order to test the applicability of a previously developed kinetic model through all the crystallization range between T_g and T_m^0. The model accounts for expressions for the induction time and for the temperature dependence of the kinetic constant. Moreover, a more rigorous approach to represent the temperature dependence of the kinetic constant was used to allow a more precise parameters calculation. The proposed set of equations was able to describe the crystallization process even at very fast cooling rates close to the region of partial and total quenching of the polymer. And a comparison of the Nakamura and Kamal model for the dynamic crystallization showed that the former represents the behavior of New TPI in a better way.

The results of the crystallization kinetics were used to build time–temperature transformation and constant cooling transformation plots that are proposed as a useful tool for the processing of semicrystalline polymers and for a better understanding of their crystallization behavior.

The authors would like to acknowledge Prof. L. Nicolais from the University of Naples and Prof. J. Seferis from the University of Washington for their useful advice.

REFERENCES

1. B. Wunderlich, *Macromolecular Physics,* Vol. 2, Academic Press, New York, 1976.
2. J. D. Hoffman, G. T. Davis, and J. I. Lauritzen, in *Treatise on Solid State Chemistry,* Vol. 3, N. B. Hannay, Ed., Plenum Press, New York, 1976, Chap. 7.
3. G. P. Desio and L. Rebenfeld, *J. Appl. Polym. Sci.,* **44,** 1989 (1992).
4. G. P. Desio and L. Rebenfeld, *J. Appl. Polym. Sci.,* **44,** 2005 (1992).
5. J. M. Kenny and A. Maffezzoli, *Polym. Eng. Sci.,* **31,** 607 (1991).
6. N. A. Mehl and L. Rebenfeld, *J. Polym. Sci., Polym. Phys.,* **31,** 1677 (1993).
7. A. Maffezzoli, J. M. Kenny, and L. Nicolais, *J. Mater. Sci.,* **28,** 4994 (1993).
8. J. M. Kenny, A. Maffezzoli, and L. Nicolais, *Thermochim. Acta,* **227,** 83 (1993).
9. V. Brucato, G. Crippa, S. Piccarolo, and G. Titomanlio, *Polym. Eng. Sci.,* **31,** 1411 (1991).
10. R. Patel and J. E. Spruiell, *Polym. Eng. Sci.,* **31,** 730 (1991).
11. P. Cebe, *Polym. Eng. Sci.,* **28,** 1192 (1988).
12. L. C. Lopez and G. L. Wilkes, *Polymer,* **29,** 106 (1988).
13. D. Progar, T. St. Clair, H. Burks, C. Gatreux, A. Yamaguchi, and M. Oshita, *Sampe J.,* **26,** 53 (1989).
14. F. W. Harrys, M. W. Belz, and P. M. Hergenrother, *Sampe J.,* **23,** 6 (1987).
15. A. Yamaguchi and Oshita, *Sampe J.,* **23,** 28 (1987).
16. T. H. Hou and R. M. Reddy, *Sampe Quart.,* **22,** 38 (1991).
17. P. P. Huo, J. B. Friler, and P. Cebe, *Polymer,* **34,** 4387 (1993).
18. J. B. Friler and P. Cebe, *Polym. Eng. Sci.,* **33,** 587 (1993).

19. J. M. Kenny, A. Maffezzoli, and L. Nicolais, *Polym. Compos.*, **5,** 1 (1992).
20. M. Ward, *Mechanical Properties of Solid Polymers,* John Wiley & Sons, 1971.
21. M. R. Kamal and E. Chu, *Polym. Eng. Sci.,* **23,** 27 (1983).
22. C. C. Lin, *Polym. Eng. Sci.,* **23,** 113 (1983).
23. K. Nakamura, K. Katayama, and T. Amano, *J. Appl. Polym. Sci.,* **17,** 1031 (1973).
24. C. Velisaris and J. C. Seferis, *Polym. Eng. Sci.,* **26,** 1574 (1986).
25. L. H. Van Vlack, *Elements of Material Science,* 2nd ed., Addison–Wesley, Reading, MA, 1964.
26. J. B. Enns and J. K. Gillham, *J. Appl. Polym. Sci.,* **28,** 2567 (1983).

Received August 4, 1994
Accepted November 7, 1994